

Rapid ratiometric determination of hemoglobin concentration using UV-VIS diffuse reflectance at isosbestic wavelengths

Janelle E. Phelps,^{1,*} Karthik Vishwanath,¹ Vivide T. C. Chang,¹ and Nirmala Ramanujam¹

¹Department of Biomedical Engineering, Duke University, 136 Hudson Hall, Box 90281, Durham, NC 27708, USA
[*janelle.bender@duke.edu](mailto:janelle.bender@duke.edu)

Abstract: We developed a ratiometric method capable of estimating total hemoglobin concentration from optically measured diffuse reflectance spectra. The three isosbestic wavelength ratio pairs that best correlated to total hemoglobin concentration independent of saturation and scattering were 545/390, 452/390, and 529/390 nm. These wavelength pairs were selected using forward Monte Carlo simulations which were used to extract hemoglobin concentration from experimental phantom measurements. Linear regression coefficients from the simulated data were directly applied to the phantom data, by calibrating for instrument throughput using a single phantom. Phantoms with variable scattering and hemoglobin saturation were tested with two different instruments, and the average percent errors between the expected and ratiometrically-extracted hemoglobin concentration were as low as 6.3%. A correlation of $r = 0.88$ between hemoglobin concentration extracted using the 529/390 nm isosbestic ratio and a scalable inverse Monte Carlo model was achieved for *in vivo* dysplastic cervical measurements (hemoglobin concentrations have been shown to be diagnostic for the detection of cervical pre-cancer by our group). These results indicate that use of such a simple ratiometric method has the potential to be used in clinical applications where tissue hemoglobin concentrations need to be rapidly quantified *in vivo*.

©2010 Optical Society of America

OCIS codes: (170.6510) Spectroscopy, tissue diagnostics; (170.1470) Blood or constituent monitoring.

References and links

1. W. Tjalma, E. Van Marck, J. Weyler, L. Dirix, A. Van Daele, G. Goovaerts, G. Albertyn, and P. van Dam, "Quantification and prognostic relevance of angiogenic parameters in invasive cervical cancer," *Br. J. Cancer* **78**(2), 170–174 (1998).
2. J. S. Lee, H. S. Kim, J. J. Jung, M. C. Lee, and C. S. Park, "Angiogenesis, cell proliferation and apoptosis in progression of cervical neoplasia," *Anal. Quant. Cytol. Histol.* **24**(2), 103–113 (2002).
3. N. Weidner, P. R. Carroll, J. Flax, W. Blumenfeld, and J. Folkman, "Tumor angiogenesis correlates with metastasis in invasive prostate carcinoma," *Am. J. Pathol.* **143**(2), 401–409 (1993).
4. J. F. Jansen, J. A. Koutcher, and A. Shukla-Dave, "Non-invasive imaging of angiogenesis in head and neck squamous cell carcinoma," *Angiogenesis* (2010).
5. K. Maeda, Y. S. Chung, S. Takatsuka, Y. Ogawa, T. Sawada, Y. Yamashita, N. Onoda, Y. Kato, A. Nitta, Y. Arimoto, Y. Kondo, and M. Sowa, "Tumor angiogenesis as a predictor of recurrence in gastric carcinoma," *J. Clin. Oncol.* **13**(2), 477–481 (1995).
6. S. C. Vieira, L. C. Zeferino, B. B. Da Silva, G. Aparecida Pinto, J. Vassallo, G. A. Carasan, and N. G. De Moraes, "Quantification of angiogenesis in cervical cancer: a comparison among three endothelial cell markers," *Gynecol. Oncol.* **93**(1), 121–124 (2004).
7. T. J. Farrell, M. S. Patterson, and B. Wilson, "A diffusion theory model of spatially resolved, steady-state diffuse reflectance for the noninvasive determination of tissue optical properties *in vivo*," *Med. Phys.* **19**(4), 879–888 (1992).
8. G. M. Palmer, and N. Ramanujam, "Monte Carlo-based inverse model for calculating tissue optical properties. Part I: Theory and validation on synthetic phantoms," *Appl. Opt.* **45**(5), 1062–1071 (2006).

9. G. M. Palmer, C. Zhu, T. M. Breslin, F. Xu, K. W. Gilchrist, and N. Ramanujam, "Monte Carlo-based inverse model for calculating tissue optical properties. Part II: Application to breast cancer diagnosis," *Appl. Opt.* **45**(5), 1072–1078 (2006).
10. L. Wang, S. L. Jacques, and L. Zheng, "MCML--Monte Carlo modeling of light transport in multi-layered tissues," *Comput. Methods Programs Biomed.* **47**(2), 131–146 (1995).
11. M. L. Ellsworth, R. N. Pittman, and C. G. Ellis, "Measurement of hemoglobin oxygen saturation in capillaries," *Am. J. Physiol.* **252**(5 Pt 2), H1031–H1040 (1987).
12. R. N. Pittman, and B. R. Duling, "A new method for the measurement of percent oxyhemoglobin," *J. Appl. Physiol.* **38**(2), 315–320 (1975).
13. Q. Liu, and T. Vo-Dinh, "Spectral filtering modulation method for estimation of hemoglobin concentration and oxygenation based on a single fluorescence emission spectrum in tissue phantoms," *Med. Phys.* **36**(10), 4819–4829 (2009).
14. J. E. Bender, K. Vishwanath, L. K. Moore, J. Q. Brown, V. Chang, G. M. Palmer, and N. Ramanujam, "A robust Monte Carlo model for the extraction of biological absorption and scattering *in vivo*," *IEEE Trans. Biomed. Eng.* **56**(4), 960–968 (2009).
15. G. M. Palmer, C. Zhu, T. M. Breslin, F. Xu, K. W. Gilchrist, and N. Ramanujam, "Comparison of multiexcitation fluorescence and diffuse reflectance spectroscopy for the diagnosis of breast cancer (March 2003)," *IEEE Trans. Biomed. Eng.* **50**(11), 1233–1242 (2003).
16. S. Prahl, "Optical Properties Spectra," (Oregon Medical Laser Center, 2003).
17. S. Prahl, "Mie Scattering Program," (Oregon Medical Laser Center, 2005).
18. J. E. Bender, A. B. Shang, E. W. Moretti, B. Yu, L. M. Richards, and N. Ramanujam, "Noninvasive monitoring of tissue hemoglobin using UV-VIS diffuse reflectance spectroscopy: a pilot study," *Opt. Express* **17**(26), 23396–23409 (2009).
19. T. M. Bydlon, S. A. Kennedy, L. M. Richards, J. Q. Brown, B. Yu, M. K. Junker, J. Gallagher, J. Geradts, L. G. Wilke, and N. Ramanujam, "Performance metrics of an optical spectral imaging system for intra-operative assessment of breast tumor margins," *Opt. Express* **18**(8), 8058–8076 (2010).
20. J. R. Mourant, T. Fuselier, J. Boyer, T. M. Johnson, and I. J. Bigio, "Predictions and measurements of scattering and absorption over broad wavelength ranges in tissue phantoms," *Appl. Opt.* **36**(4), 949–957 (1997).
21. R. Reif, M. S. Amoroso, K. W. Calabro, O. A' Amar, S. K. Singh, and I. J. Bigio, "Analysis of changes in reflectance measurements on biological tissues subjected to different probe pressures," *J. Biomed. Opt.* **13**(1), 010502 (2008).
22. V. T. Chang, P. S. Cartwright, S. M. Bean, G. M. Palmer, R. C. Bentley, and N. Ramanujam, "Quantitative physiology of the precancerous cervix *in vivo* through optical spectroscopy," *Neoplasia* **11**(4), 325–332 (2009).

1. Introduction

Hemoglobin (Hb) concentration is a metric used for many applications in the medical field, including anemia diagnosis and transfusion guidance. The current strategy for determining Hb concentration is an invasive procedure where blood is drawn from an artery and sent to a laboratory for further analysis. This process is time-consuming, subject to operator error, and carries the risk of infection. Therefore the need exists for a noninvasive technique that can rapidly and accurately predict Hb concentration in human and/or animal tissues. If such a device and method were portable, it would have wide applicability in various areas where rapid Hb measurements are required, such as in the emergency or operating room, in the back of an ambulance, in the battlefield, and in other resource-limited settings.

Hb concentration can also serve as a surrogate marker for neovascularization. In cervical dysplasia, neovascularization has been shown to be associated with poor prognosis and is considered a pathoanatomic feature indicative of a greater risk of recurrence and death [1,2]. Early angiogenic changes are also indicative of neoplastic changes in different organ sites, including the prostate [3], head and neck [4], and gastrointestinal systems [5]. Characterization of neovascularization has mostly been performed by invasive and tissue destructive immunohistochemistry on formaldehyde-fixed and paraffin-embedded tissues using various antibodies [6]. Ratiometric optical spectroscopy could be used to provide noninvasive longitudinal monitoring of neovascularization.

Optical methods show a high degree of accuracy in measuring Hb concentration, but they generally require a sophisticated computational technique such as diffusion approximation [7] or Monte Carlo modeling [8–10] to extract this information from the measured spectra. The focus of the present study is to use simple diffuse reflectance ratios to determine Hb concentration. Optical ratiometric methods involve measurements of reflectance and/or fluorescence at two or more wavelength points to produce a functional form which is subsequently shown to be correlated with a given physical parameter. Oxy- and deoxy-Hb

have eight isosbestic points in the ultraviolet-visible (UV-VIS) wavelength range. Isosbestic points indicate wavelengths where two chemical species have the same molar extinction coefficient. Because Hb saturation is calculated from the ratio of oxy-Hb to total Hb, measurements taken at isosbestic points are independent of saturation. Studies from the literature have used ratios involving both isosbestic and non-isosbestic points as a metric to quantify Hb saturation [11,12] and Hb concentration [13].

Several studies in the literature have capitalized on isosbestic points to measure Hb saturation, by using a ratio consisting of one isosbestic point and one where there are maximal differences between oxy- and deoxy-Hb. In one study, a microdensitometer was used to measure oxygen saturation in capillaries of the hamster cheek pouch, through the use of a ratio including the 420 nm isosbestic point and 431 nm non-isosbestic point [11]. Other studies have used ratios involving two or more isosbestic wavelengths of Hb. One study used 520 and 546 nm to determine the contribution of scattering to optical density measurements of whole blood [12]. The scattering term could then be used to calculate Hb absorption at the two isosbestic points plus a third wavelength where the oxy- and deoxy-Hb extinction coefficients were different. This, in turn could then be used to calculate Hb saturation. Another study using fluorescence emission measurements from phantoms comprised of flavin adenine dinucleotide, Hb, and polystyrene spheres, found the ratio of fluorescence intensity at two isosbestic points, 500 and 570 nm, could be used to measure total Hb concentration. This ratio was independent of scattering and Hb saturation [13]. Furthermore, the authors determined that the ratio calculated as the product of 540/560 and 578/560 nm was related to Hb saturation. It is evident from the literature that there is a push towards the development of simple algorithms to measure biologically relevant optical parameters, such as total Hb concentration.

The focus of this present study is to assess the accuracy of total Hb estimation, independent of Hb saturation and scattering, using a simple isosbestic ratiometric analysis of diffuse reflectance intensities developed using Monte Carlo simulations, and whose accuracy was assessed using tissue-mimicking phantoms and *in vivo* human cervical precancer data. Diffuse reflectance spectra were generated using a forward Monte Carlo model, then equations of linear regression between Hb concentration and the ratios were established from the simulations and applied to phantom data. A single reference phantom was used to calibrate the Monte Carlo-generated reflectance to the same scale as the experimentally-measured data. The simulation equations were specific to the probe and instrument used experimentally.

Simulations were conducted for five scattering levels for each of ten absorption levels (Hb concentrations). There were 28 total ratios tested for isosbestic points between 350 and 600 nm. A simple analytical equation was developed to predict Hb concentration. Twenty-five of the 28 ratios had average percent errors within 20% for the simulations when the ratios were averaged over all five scattering levels, four of which were below 5%, nine of which were between 5 and 10%, and seven of which were between 10 and 15%. Linear regression equations from the simulations were then applied to three sets of experimental phantom data. Of the 25 best ratios from the simulations, 12 ratios yielded average percent error within a 20% threshold in extracting Hb concentration from phantoms (Phantom Set 1) with constant Hb concentration and scattering, but variable Hb saturation. Seven of these ratios had errors below 5%, two had errors between 5 and 10%, and three had errors between 15 and 20%. From these 12 ratios, there were a total of six ratios (545/390, 452/390, 570/390, 529/390, 584/390, and 500/390) which could extract Hb concentration from two sets of phantoms (Phantom Sets 2 and 3) with variable Hb concentration and scattering with errors below a 20% threshold. For 452/390 nm, the average percent error was below 15% for both phantom sets. For Phantom Set 2, the average percent error was below 10% for 452/390 nm, between 10 and 15% for 529/390 and 500/390 nm, and between 15 and 20% for 545/390, 570/390, and 584/390 nm. For Phantom Set 3, the average percent error was between 10 and 15% for 545/390, 452/390, 570/390, and 584/390 nm and between 15 and 20% for 529/390 and 500/390 nm.

In order to assess the instrument-independence of this ratiometric method, the six best ratios were tested for two sets of phantoms with variable scattering and Hb concentration measured with a second instrument that used a photomultiplier tube rather than charge-coupled device as the detector. Three of these ratios – 545/390, 452/390, and 529/390 nm – had similarly low errors within 20%, indicating this method can be considered independent of the instrument and probe used. Data from human cervical measurements measured with both instruments was used to test the correlations with Hb concentration extracted with either the ratiometric method or a more complex inverse Monte Carlo model previously developed and validated by our lab [8,14,15]. Both the inverse Monte Carlo model and ratiometric method extracted a wide range of Hb concentration with Pearson linear correlation coefficients of 0.75, 0.76, and 0.88 for the three best ratios, 545/390, 452/390, and 529/390 nm, respectively

2. Materials and methods

The goal of this study was to identify a set of isosbestic ratios that were best correlated to Hb concentration independent of scattering and Hb saturation. Figure 1 is a flowchart summarizing the steps taken to determine and test the best ratio(s).

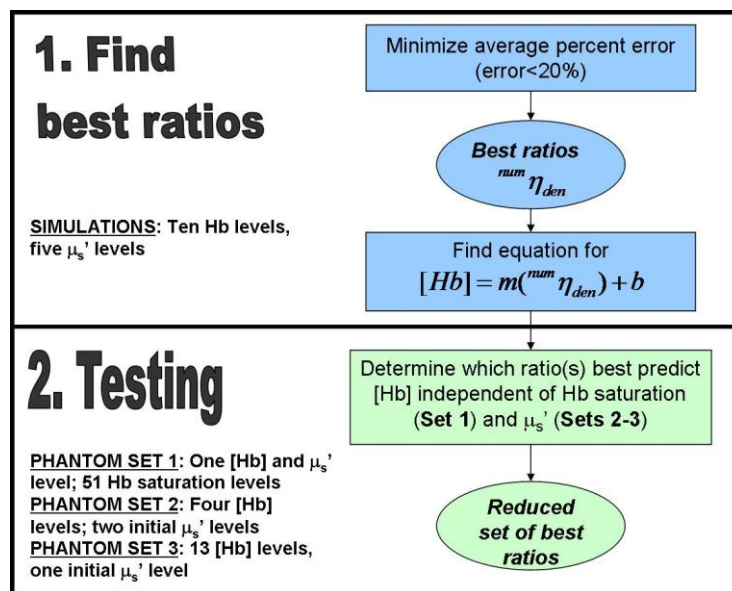


Fig. 1. Flow chart illustrating the processes for selecting the best ratios which were tested in three sets of phantoms.

The simulations consisted of 50 tissue models, with five scattering levels for each of ten absorption levels. Upon determining the best ratios, designated in the flow chart by ${}^{num}\eta_{den}$, where num is the numerator and den the denominator, tissue-mimicking phantoms were used for testing the linear regression equations developed from the simulations. Because the testing was conducted using the linear regression equations derived directly from the simulations, no training on tissue phantoms was required. The three sets of phantoms were designed to test the independence of the ratiometric method to Hb saturation (Set 1) and scattering (Sets 2-3). Phantom Set 1 contained 51 phantoms with variable Hb saturation and constant Hb concentration and scattering. Phantom Set 2 had four Hb levels for two initial scattering levels which decreased slightly due to addition of Hb. Phantom Set 3 consisted of 13 Hb levels for a single initial scattering level which decreased to a greater extent due to addition of Hb. A subset of ratios was tested for Phantom Sets 2 and 3, based upon the best ratio(s) from Phantom Set 1. A new set of ratios was then selected and tested on Phantom Sets 2 and 3 measured with a different instrument, to establish that this method was independent of

instrument response. Upon determining the best ratio(s), the extraction ability of Hb concentration was compared between this ratiometric approach and a scalable inverse Monte Carlo model [8] developed by our group on in vivo diffuse reflectance measurements from cervical tissues.

2.1 Determination of the best ratios using Monte Carlo simulations

Forward Monte Carlo simulations [8] were conducted to determine the best isosbestic ratios of oxy- and deoxy-Hb that could predict Hb concentration. There are eight isosbestic points for oxy- and deoxy-Hb over the 350-600 nm wavelength range: 390, 422, 452, 500, 529, 545, 570, and 584 nm [16]. Combinations of ten absorption and five scattering levels were used to generate optical property inputs to the 400 simulated tissue models (10 Hb levels, 5 scattering levels, 8 wavelengths). The absorption levels (Table 1) corresponded to total Hb concentrations of 5-50 μM with different fractions of oxy- and deoxy-Hb (thus different Hb saturations). The absorption coefficient (μ_a) at each isosbestic wavelength was determined using the molar extinction coefficients for each hemoglobin species [16].

Table 1. Total Hb concentration and Hb saturation used in the simulations

[Total Hb] (μM)	Hb saturation (%)
5	50
10	100
15	66.7
20	25
25	80
30	50
35	85.7
40	62.5
45	77.8
50	100

Five different scattering levels, S1-S5 (Table 2), were combined with each of the absorption levels. The reduced scattering coefficient (μ_s') at each of the eight isosbestic wavelengths was calculated using freely available Mie theory software [17]. For a given wavelength pair, the ratio of scattering was independent of the scattering level. The choices of absorption and scattering levels were made based on previous studies conducted by our lab [14,18].

Table 2. μ_s' for each of the five scattering levels as a function of isosbestic wavelength

Wavelength (nm)	S1 (cm^{-1})	S2 (cm^{-1})	S3 (cm^{-1})	S4 (cm^{-1})	S5 (cm^{-1})
390	10.0	15.0	20.1	25.0	30.0
422	9.4	14.1	18.8	23.4	28.1
452	9.0	13.5	18.0	22.5	27.0
500	8.4	12.5	16.7	20.9	25.0
529	8.1	12.1	16.1	20.1	24.2
545	8.0	12.0	16.0	20.0	24.0
570	7.9	11.8	15.8	19.6	23.6
584	7.7	11.5	15.4	19.2	23.0

The simulations were scaled for the exact probe geometry used in the experimental measurements on which the ratios were tested. The scaling process used an image of the common end of the fiber probe and has been discussed previously [8,14]. The probe geometry consisted of a central illumination core of 18 illumination fibers surrounded by 19 collection fibers in a concentric arrangement, with each individual fiber being 200 μm in diameter with numerical aperture (NA) of 0.22. The approximate spatial resolution of this probe is 1 mm, as determined by the full-width at half maximum of the collected fraction versus source detector separation distance. The collected fraction was determined from convolution over the illumination and collection fibers as described in [8]. The average 90% sensing depth over 350-600 nm is approximately 2.2 ± 0.7 mm [18]. For all tissue models, the anisotropy factor, g , was 0.8, and the refractive indices for the fibers and tissue were at 1.45 and 1.37,

respectively [18,19]. From the forward Monte Carlo model, the diffuse reflectance was determined using a lookup table method described previously [8]. Reflectance ratios were calculated from the modeled diffuse reflectance at each isosbestic point.

Determination of the best ratio: The simulations were used to determine which ratios best correlated to Hb concentration. Reflectance ratios at isosbestic wavelengths were only computed when the numerator wavelength was higher than the denominator wavelength yielding a total of 28 possible ratio combinations. The criterion for the simulation data was to minimize the goodness of fit, or the average percent error, %error, defined in Eq. (1), where n is the number of Hb levels, Hb is the concentration of Hb, and fit is the linear regression equation for Hb versus ratio:

$$\%error = 100 \cdot \frac{\sum \left| \frac{fit - Hb}{Hb} \right|}{n} \quad (1)$$

The errors were determined after the ratios were averaged over all scattering levels, and the best ratios were defined as having %error \leq 20%.

2.2 Testing on synthetic tissue-mimicking phantoms

The efficacy of isosbestic ratiometric correlations to Hb concentration was evaluated by testing on three independent sets of tissue-mimicking phantoms. The linear regression equations for the best ratios from the simulations were applied to the phantom data. In order to correct for the instrument dependence, the simulated reflectance was first calibrated by a correction factor determined using a single phantom measurement to put the Monte Carlo data and the experimental data on the same scale. Briefly, the calibration phantom was selected from a set of master phantoms that has previously been found to most accurately estimate μ_a and μ_s' over a large range of target phantom optical properties [14]. The calibration phantoms used for either instrument here had approximate absorption coefficient, $\mu_a = 2.2 \text{ cm}^{-1}$ and reduced scattering coefficient, $\mu_s' = 24.8 \text{ cm}^{-1}$, averaged over 350-600 nm. The calibration phantom can be measured prior to taking the laboratory or clinical measurements, and so the time taken to measure it is not relevant to the time it would take to estimate Hb concentration using this ratiometric method. All diffuse reflectance data from the phantoms were divided by the spectrum of a reflectance standard (Spectralon, LabSphere, North Sutton, NH) measured on the same day prior to taking the ratios, so that the ratios were calculated from the true diffuse reflectance spectrum of the interrogated medium independent of lamp and/or detector response. For the phantom measurements, the percent error was calculated from Eq. (1), where the fit refers to the extracted Hb concentration using the linear regression equation derived from calibrated simulation data. Figure 2 describes the procedure for finding the best ratios using the phantom data.

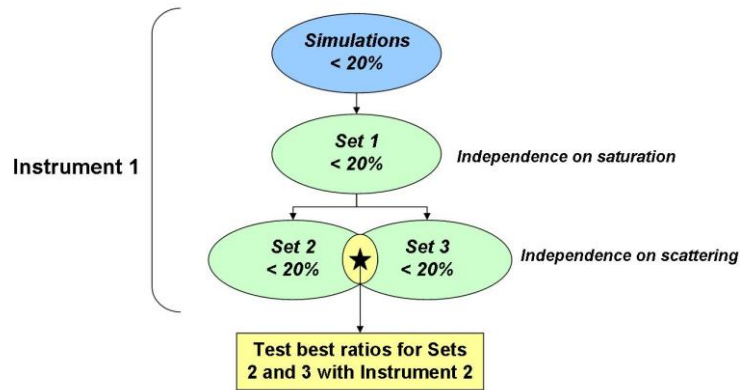


Fig. 2. Flow chart illustrating the processes for selecting the best ratios based on the phantom experiments.

Phantom Set 1 consisted of phantoms with variable levels of Hb saturation and constant Hb concentration and μ_s' . Briefly, a phantom with Hb concentration of $14.8 \mu\text{M}$ and mean μ_s' of 12.59 cm^{-1} (over 350-600 nm) was slowly desaturated, and 51 optical measurements were collected simultaneously with oxygen partial pressure ($p\text{O}_2$), as previously described [14]. A reduced set of ratios with $\% \text{error} \leq 20\%$ for Phantom Set 1 was tested by applying the regression from the simulations to Phantom Sets 2-3. Set 2 consisted of eight phantoms separated into two sets of four, where the sets refer to a lower and higher scattering level. For each set of four, Hb concentration was increased by serial additions of stock solution. Set 3 consisted of 13 phantoms, which had increasing Hb concentration for a single initial scattering level. For each of the sets, the addition of absorber caused a reduction in the scattering. The best ratios were considered those for which the $\% \text{error}$ was within 20% for both Sets 2 and 3.

To test whether the ratiometric method had any instrument-dependence, the best ratios determined from the phantom sets were tested with a second instrument. Again, the exact probe geometry was accounted for in the forward Monte Carlo model, and a single phantom was used to calibrate the experimental data for the instrument-dependence of the diffuse reflectance such that the diffuse reflectance from the phantoms and the forward Monte Carlo model were on the same scale. The phantom sets measured with the two instruments had similar absorption and scattering levels, but Set 3 for Instrument 2 was comprised of 16 phantoms covering a larger range of concentrations and thus a wider range of μ_s' levels than those measured with Instrument 1. Table 3 summarizes the absorption (Hb concentration) and scattering (mean μ_s' from 350 to 600 nm) levels of Sets 2 and 3 for each instrument. The first instrument (Instrument 1) consisted of a 450 W xenon (Xe) arc lamp (JY Horiba, Edison NJ), double-excitation monochromator (Gemini 180, JY Horiba, Edison, NJ), and Peltier-cooled open-electrode charge-coupled device (CCD) (Symphony, JY Horiba, Edison, NJ). The second instrument (Instrument 2) was a spectrophotometer (SkinSkin, JY Horiba, Edison, NJ) consisting of a 150 W Xe arc lamp, double-grating excitation monochromator, emission monochromator, and extended red photomultiplier tube (PMT). The illumination and collection light for both instruments was coupled to a fiber optic probe, which had the same illumination and collection geometry for both instruments.

Table 3. Ranges of Hb concentrations and mean μ_s' (averaged over 350-600 nm) for Phantom Sets 2 and 3. Set 2 had two μ_s' levels, each of which had the same range of Hb

	<i>Instrument 1 ranges</i>		<i>Instrument 2 ranges</i>	
	<i>[Hb] (μM)</i>	<i>Mean μ_s' (cm^{-1})</i>	<i>[Hb] (μM)</i>	<i>Mean μ_s' (cm^{-1})</i>
Set 2: μ_s' level 1 (n=4)		14.0-13.0		14.3-13.1
Set 2: μ_s' level 2 (n=4)	6.4-14.3	23.4-21.7	7.3-16.2	23.9-21.9
Set 3	5.9-35.2	23.6-17.3	5.0-50.0	27.8-17.0

2.3 Sensitivity analysis

The robustness of this method with regard to scattering slope was tested. The scattering was modeled as a power law, with $\mu_s' = a \cdot \lambda^{-b}$, where λ is wavelength, b refers to the scattering slope, and a is a scattering magnitude factor. For the μ_s' levels shown in Table 2, the value of b was approximately 0.6. Scattering slopes with values between 0.37 and 4 with an increment of 0.1 were tested, as those limits represent the range for particles much larger than the wavelength of light and the Rayleigh scattering regime, respectively [20,21]. The different scattering slopes were applied to the μ_s' values in the simulations, then new linear regression equations were derived. To apply the new scattering slopes, the values for a were determined by fitting the original μ_s' values to a power law. Then, the new values for μ_s' were calculated using new b values and the same a values determined from the original μ_s' values. Additionally the effects of using different values for g (0.7, 0.9, and 0.95) were also tested. The sensitivity analysis was only performed on data collected with Instrument 1.

2.4 Clinical applicability

The clinical applicability of isosbestic ratiometric correlations to Hb concentration was tested on *in vivo* measurements of the human cervix, which have been described in a previously published paper [22]. The study protocol was reviewed and approved by the Institutional Review Board at Duke University Medical Center (DUMC). Patients referred to the DUMC Colposcopy Clinic following an abnormal Pap smear were recruited for the study. Diffuse reflectance, delivered to and collected via a fiber optic probe, was collected from one to three visually abnormal site(s) immediately following colposcopic examination of the cervix with the application of 5% acetic acid. This was followed by an optical measurement on a colposcopically normal site from the same patient. Optical interrogation of colposcopically normal and abnormal sites was conducted prior to biopsy to avoid confounding absorption due to superficial bleeding. Diffuse reflectance from 76 sites in 38 patients were normalized by a reflectance standard and interpolated prior to calculating the reflectance ratios. Scattering, absorption, and Hb concentration were also extracted from the same data using a scalable inverse Monte Carlo model [8,14]. The instrumentation used to collect diffuse reflectance *in vivo* was identical to those described in the Section 2.2 (both Instruments 1 and 2 were used).

3. Results

3.1 Determination of the best ratios

The optical ratios were averaged over all scattering levels for a given Hb concentration in the simulations. Of the 28 total ratios, the average percent error was within 20% for 25 ratios. Figure 3 shows a histogram of the average percent errors for those 25 ratios; four ratios had %error below 5%, nine had %error between 5 and 10%, seven had %error between 10 and 15%, and five had %error between 15 and 20%. For the 25 best ratios, all slopes and intercepts were statistically different from zero, as determined from linear regression t-tests.

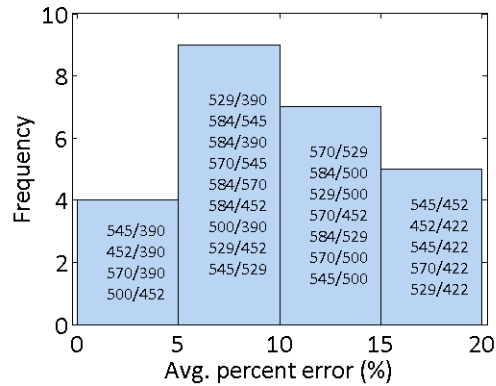


Fig. 3. Histogram of average percent errors from the simulations. The ratios within each bin of the histogram are labeled on the figure in order of increasing %error.

3.2 Testing using phantoms with variable Hb saturation

The ability to utilize ratiometric linear regression equations from the simulations to extract Hb concentration from experimentally measured phantoms with variable saturation was tested. Figure 4 shows the average percent errors for each of the 25 best ratios from the simulations. The average and standard deviations were taken over all 51 phantom measurements.

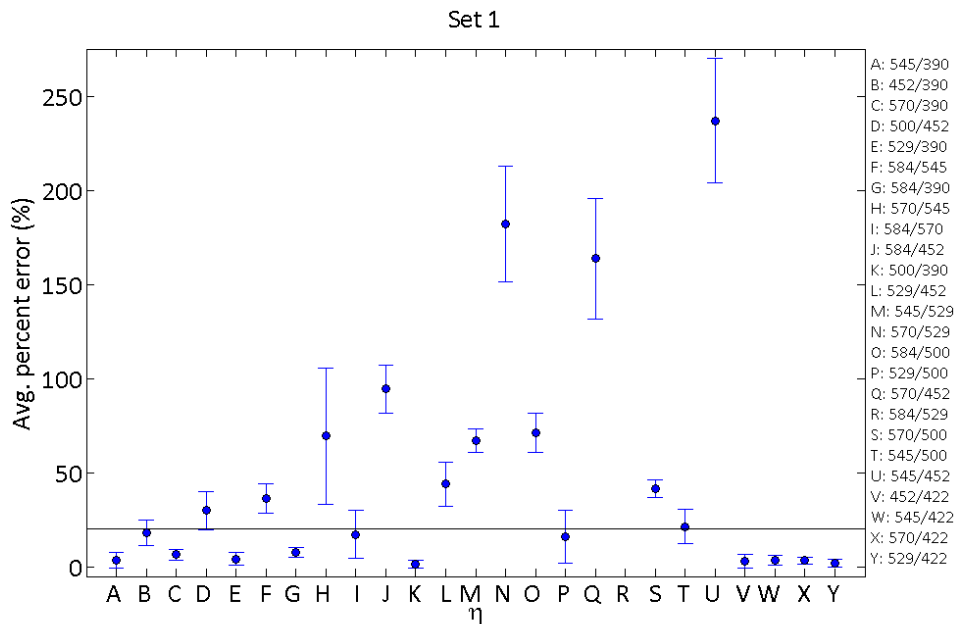


Fig. 4. Average percent error for Set 1 for each of the 25 best ratios determined from the simulations. The black line shows the cut-off of 20% average error.

There were 12 ratios with %error < 20% for the Hb saturation phantoms, seven of which had errors below 5%, two which had errors between 5 and 10%, and three of which had errors between 15 and 20%.

3.3 Testing using phantoms with variable scattering and Hb concentration

Figure 5 shows the average percent error with corresponding standard deviation for the 12 best ratios determined from Phantom Set 1. The top figure shows the results for Set 2, which had two distinct scattering levels, while the bottom figure is for Set 3, which covered a wide range of Hb concentration levels for a single scattering level.

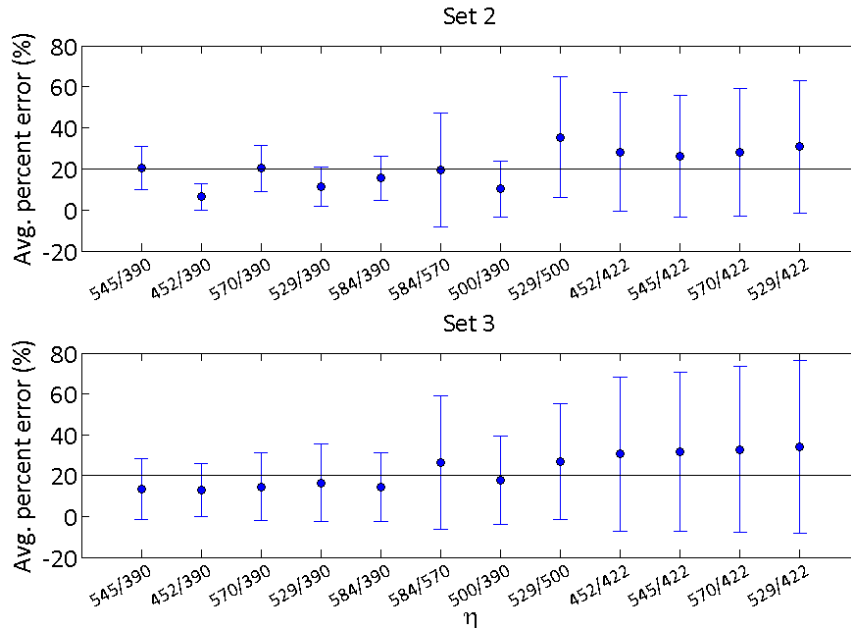


Fig. 5. Average percent error for Set 2 (top) and Set 3 (bottom) measured with Instrument 1 for each of the 12 best ratios determined from the Hb saturation phantoms. The black line shows the cut-off of 20% average error.

Set 2 had seven ratios with average percent error within 20%, while Set 3 had six. Between the two sets, there were six ratios which yielded %error within 20%: 545/390, 452/390, 570/390, 529/390, 584/390, and 500/390 nm. For Phantom Sets 1, 2, and 3, these were the only six ratios that resulted in $\leq 20\%$ error for each of the phantom sets, and so the order of the phantom set testing would not matter. The average percent error for 452/390 nm was below 15% for both phantom sets.

The six best ratios between Set 2 and 3 measured with Instrument 1 were then tested on phantom measurements using Instrument 2 (Fig. 6). Three of the ratios had percent errors within the 20% threshold for Set 2 (545/390, 452/390, and 529/390 nm), and four of the ratios did for Set 3 (545/390, 452/390, 570/390, and 529/390 nm).

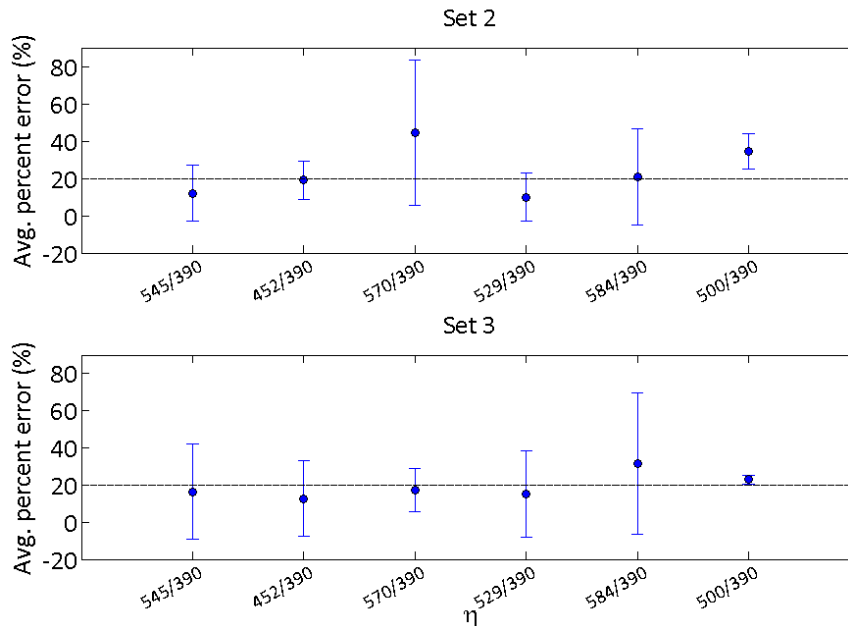


Fig. 6. Average percent error for Set 2 (top) and Set 3 (bottom) measured with Instrument 2 for each of the six best ratios determined from phantoms measured with Instrument 1. The black line shows the cut-off of 20% average error.

Table 4 shows the average percent error for the six best ratios determined from Instrument 1 for the simulations, Phantom Set 1, and Phantom Sets 2 and 3 for each instrument. The accuracy of extracting Hb concentration using the inverse Monte Carlo model [8] was also tested for Phantom Sets 2-3 measured with both instruments.

Table 4. Average percent error for the simulations (“Sims”) and three testing phantom sets. Set 1 had variable Hb saturation, Set 2 had variations in Hb concentration for two scattering levels, and Set 3 had large variations in Hb concentration for one scattering level. Sets 2 and 3 were measured with both instruments. The errors are shown for the six best ratios and the inverse Monte Carlo model

%error		545/390	452/390	570/390	529/390	584/390	500/390	Monte Carlo
Sims		2.3	2.8	3.9	5.3	5.7	9.2	-
	Set 1	3.8	18.2	6.5	4.3	7.7	1.6	-
Inst. 1	Set 2	20.4	6.3	20.3	11.4	15.5	10.2	6.7
	Set 3	13.3	12.8	14.5	16.5	14.3	17.8	7.9
Inst. 2	Set 2	12.1	19.1	44.6	9.9	20.7	34.4	3.8
	Set 3	16.5	12.7	17.4	15.2	31.7	22.8	6.1

The three ratios with errors below 20% for simulations and phantoms measured with both instruments (545/390, 452/390, and 529/390 nm) were applied to the diffuse reflectance measurements from human cervical tissues as described in Section 3.5.

3.4 Sensitivity analysis

The ranges of b for which each of the six best ratios still yielded within 20% error for simulations and Sets 1-3 when measured with Instrument 1 are shown in Table 5. The “best ratios” here were considered ones which had resulted in $\leq 20\%$ error when they were tested on both Phantom Sets 2 and 3 measured with Instrument 1. Beyond $b = 0.83$, no ratios gave within 20% error. At the low end of possible scattering slopes (0.37), only 500/390 nm had errors within 20%.

Table 5. Ranges of scattering slope, b , for which the six best ratios were still considered best ratios. To still be considered a best ratio, these values of b had to result in $\leq 20\%$ error for simulations and Sets 1-3 measured with Instrument 1

	545/390	452/390	570/390	529/390	584/390	500/390
b range	0.67-0.8	0.57-0.8	0.64-0.83	0.55-0.78	0.59-0.79	0.37-0.68

When different values of g were tested, all phantom sets measured with Instrument 1 generally maintained an error within 20%. The average percent errors are shown in Table 6 for Sets 1-3 measured with Instrument 1.

Table 6. Average percent error when $g = 0.7, 0.9$, and 0.95 were used for Sets 1-3 measured with Instrument 1. The average percent error for 545/390 and 570/390 nm with Set 2 and $g = 0.7$ slightly exceeded the 20% limit

	%error	545/390	452/390	570/390	529/390	584/390	500/390
Set 1	$g=0.7$	4.8	16.9	8.4	3.4	9.5	2.2
	$g=0.9$	3.5	19.5	4.6	5.7	5.8	1.8
	$g=0.95$	3.5	19.8	4.0	6.3	5.1	2.0
Set 2	$g=0.7$	23.2	5.4	22.0	13.0	15.6	17.2
	$g=0.9$	18.3	7.6	18.5	9.9	13.8	10.9
	$g=0.95$	17.5	8.2	17.7	9.3	13.1	11.3
Set 3	$g=0.7$	12.3	11.8	13.5	15.6	13.4	17.2
	$g=0.9$	14.4	13.8	15.5	17.4	15.2	18.4
	$g=0.95$	14.9	14.2	16.0	17.8	15.7	18.7

3.5 Clinical applicability

Data measured from an *in vivo* dysplastic cervical study were used to test the correlations between ratiometrically-extracted Hb and Hb extracted with the inverse Monte Carlo model [8]. Briefly, a reference phantom was used to put the Monte Carlo-generated and experimentally measured data on the same scale. The Pearson linear correlations between the ratiometrically- and Monte Carlo-extracted Hb were 0.75, 0.76, and 0.88 for 545/390, 452/390, and 529/390 nm, respectively. Figure 7 shows the ratio-extracted versus Monte Carlo-extracted Hb for each of the three ratios for all 76 *in vivo* measurements.

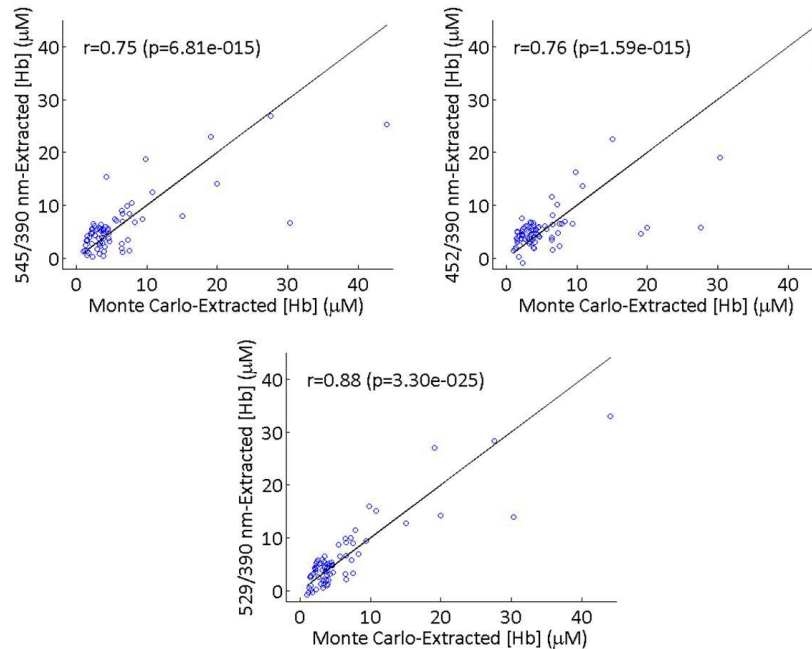


Fig. 7. Monte Carlo-extracted Hb versus Hb extracted with 545/390 (top left), 452/390 (top right), and 529/390 nm (bottom) reflectance ratios for *in vivo* cervical measurements. The solid line is the line of perfect agreement for the Monte Carlo-extracted Hb concentration.

4. Discussion

We have developed an algorithm that can be used to predict the concentration of hemoglobin using simple isosbestic ratios of diffuse reflectance spectra. This algorithm employs linear regression equations from Monte Carlo simulations which were modeled for the exact probe geometry used in the experimental measurements. The linear regression equations from the simulations were determined from instrument-calibrated diffuse reflectance and could be directly applied to the experimental spectral data. Only one phantom was required to put the measured reflectance on the same scale as the Monte Carlo-generated reflectance, and this phantom only has to be measured one time for any instrument-probe combination. Based on the simulations and tissue-mimicking phantom studies, a set of three isosbestic ratios was determined to be best correlated to Hb concentration: 545/390, 452/390, and 529/390 nm.

One caveat of this method was that when Hb concentration levels below 5 μM were used for the phantom testing, the errors increased such that only one ratio (452/390 nm) was within the 20% error limit for Phantom Sets 2-3 measured with Instrument 1 (data not shown). Because the simulations had Hb concentrations starting at 5 μM , the lower levels in the phantoms were omitted from the analysis. While the simulations showed very low errors, there were some increases in error with the phantoms. This method will be tested on additional phantom sets, because as with any laboratory experiment, there are several sources of potential errors in the preparation of phantoms that can reduce the accuracy of the results. These sources of error include pipetting and ensuring the phantom and stock solutions remain thoroughly mixed.

In a previous publication, we showed that the intercept determined from linear regression of the 529/500 nm isosbestic ratio with Hb concentration was similar to the ratio of scattering at the two wavelengths (i.e. $\mu_s'(529 \text{ nm}):\mu_s'(500 \text{ nm})$) [18]. For the three best ratios of 545/390, 452/390, and 529/390 nm, the corresponding ratios of μ_s' were 0.80, 0.90, and 0.80, respectively. The intercepts determined from linear regression averaged over the five scattering levels were 0.84 ± 0.07 , 0.93 ± 0.05 , and 0.72 ± 0.1 for the three ratios,

respectively, indicating excellent agreement between the intercepts and μ_s' ratios for 545/390 and 452/390 nm. For 529/390 nm, when the lowest two scattering levels were omitted, the average intercept was 0.80 ± 0.06 , which indicates this ratio is more sensitive to scattering than the other two ratios. This dependence on scattering can be seen from the average percent errors shown in Fig. 3, where the error for 529/390 was higher than the errors for 545/390 and 452/390 nm.

Previous work has been focused on empirical determination of one or two ratios that could be used to estimate Hb concentration or Hb saturation. Here we provide three ratios that show feasibility for predicting Hb concentration in laboratory phantom and clinical *in vivo* measurements using regression equations generated from simulated data. Any one of the three ratios can be used to predict Hb concentration, which is useful in any application where rapid quantitative measurements are needed, such as in the operating room. In addition, this provides Hb concentrations that are concordant with those extracted using a more sophisticated inverse Monte Carlo model. The ratiometric approach significantly reduces the time for data processing by almost a factor of 2000 when compared to more sophisticated methods for extracting Hb concentration, such as the inverse Monte Carlo model developed by our group [8].

5. Conclusions

Diffuse reflectance measurements from Monte Carlo simulations were used to develop linear regression equations for a set of isosbestic ratios that could quantify Hb concentration from tissue mimicking phantoms and cervical precancer data. These ratios were generally independent of scattering and Hb saturation for a large range of Hb concentrations. A simple ratiometric algorithm for diffuse reflectance measurements has applicability in settings where Hb concentration needs to be measured rapidly.

Acknowledgements

K. V. would like to acknowledge support from the National Institutes of Health grant no. 1K99CA140783-01A1.